

DEVICE-CIRCUIT CO-DESIGN OF NOVEL FinFET-BASED DEVICES FOR NEUROMOR- PHIC COMPUTING AND NON-VOLATILE MEMORY APPLICATIONS



**Thesis submitted in partial fulfillment
for the Award of Degree**

DOCTOR OF PHILOSOPHY

BY

ROOPESH SINGH

**DEPARTMENT OF ELECTRONICS ENGINEERING
INDIAN INSTITUTE OF TECHNOLOGY
(BANARAS HINDU UNIVERSITY)
VARANASI-221005, INDIA**

ROLL No.20091503

2025

**DEDICATED TO LORD SHIVA & SANKATMOCHANA
FOR THE SUPREMACY AND TO THE REDEEMER OF MY SOUL**

**DEDICATED TO MY FAMILY
FOR THEIR ENDLESS LOVE, SUPPORT, AND ENCOURAGEMENT**


**DEDICATED TO MY SUPERVISORS
FOR THEIR ENDLESS MOTIVATION, ENCOURAGEMENT, AND
TEACHING SKILLS**

CERTIFICATE

It is certified that the work contained in the thesis entitled "**Device-circuit Co-design of Novel FinFET-based Devices for Neuromorphic Computing and Non-Volatile Memory Applications**" by "**Roopesh Singh**" has been carried out under my supervision and that this work has not been submitted elsewhere for a degree.

It is further certified that the student has fulfilled all the requirements of Comprehensive Examination, Candidacy, and SOTA for the award of Ph.D. Degree.

Dr. Shivam Verma



(Supervisor)

Department of Electronics Engineering
IIT(BHU), Varanasi, India, 221005



Signature of Head of Department
Department of Electronics Engineering
IIT (BHU), Varanasi, India, 221005

इलेक्ट्रॉनिकी अभियन्त्रिकी विभाग
Department of Electronics Engineering

भारतीय प्रौद्योगिकी संस्थान
Indian Institute of Technology

(बनारस हिन्दू यूनिवर्सिटी)
(Banaras Hindu University)

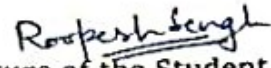
वाराणसी/Varanasi-221005

21/03/25

DECLARATION BY THE CANDIDATE

I, "**ROOPESH SINGH**," certify that the work embodied in this thesis is my own bona fide work and carried out by me under the supervision of **DR. SHIVAM VERMA** from 2020 to 2025 at the **Department of Electronics Engineering, Indian Institute of Technology (BHU), Varanasi**. The matter embodied in this thesis has not been submitted for the award of any other degree/diploma elsewhere. I declare that I have faithfully acknowledged and accredited to the research communities wherever their works have been cited in the accomplished of this thesis. I further declare that I have not intentionally copied any other's work, paragraphs, text, data, results, etc., reported in journals, books, magazines, reports, dissertations, theses, etc., or available at websites and have not included them in this thesis or cited as my own work.


Date: 21/03/2025
Place: VARANASI


Signature of the Student
ROOPESH SINGH

CERTIFICATE BY THE SUPERVISORS

It is certified that the above statement made by the student is correct to the best of my/our knowledge.


विभागाध्यक्ष/Head of the Department
इलेक्ट्रॉनिक्स अभियांत्रिकी विभाग
Department of Electronics Engineering
भारतीय प्रौद्योगिकी संस्थान
Indian Institute of Technology
(बनारस हिन्दू यूनिवर्सिटी)
(Banaras Hindu University)
वाराणसी/Varanasi-221005
25/03/25


Dr. Shivam Verma
(Supervisor)
Department of Electronics
Engineering IIT(BHU), Varanasi,
India, 221005
सहायक आचार्य/Assistant Professor
इलेक्ट्रॉनिक्स अभियांत्रिकी विभाग
Department of Electronics Engineering
भारतीय प्रौद्योगिकी संस्थान
Indian Institute of Technology
(बनारस हिन्दू यूनिवर्सिटी)
(Banaras Hindu University)
वाराणसी/Varanasi-221005

COPYRIGHT TRANSFER

The undersigned hereby assigns to the *Indian Institute of Technology (Banaras Hindu University), Varanasi, India*, all rights under copyright that may exist in and for the above thesis submitted for the award of the *Doctor of Philosophy*.

Date:21-03-2025

Place: VARANASI

A handwritten signature in blue ink that reads "Roopesh Singh". The name "Roopesh" is written in a cursive style, and "Singh" is written in a more upright, slightly cursive style. There are two horizontal lines under the "Singh" part of the signature.

Signature of the Student

ROOPESH SINGH

Note: However, the author may reproduce or authorize others to reproduce material extracted verbatim from the thesis or derivative of the thesis for the author's personal use provided that the source and the Institute's copyright notice are indicated.

ACKNOWLEDGMENT

I thank the Almighty for giving me strength and showering his blessings to bring my research investigations to a logical end successfully.

This thesis is the loveliest project I have ever worked on and has indeed been an exciting journey. It condenses all the education and inspiration I have had before and is a good compilation of my quest for the concept of spintronics devices. My gratitude cannot be expressed in words to all those who have guided, inspired, and supported me along the journey to accomplish this great achievement. I would like to express my special thanks to my supervisor Dr. Shivam Verma, whose supervision has helped me to streamline my research activities toward an intended conclusion. His advice and guidance are critical and inspiring, while his firm belief in each student's passion and potential has helped me in securing faith in this thesis from embarkment to sailing in numerous possibilities. I am grateful to have received the encouragement needed to experiment and drive my work beyond its limits. His dynamism, vision, sincerity, and motivation have deeply influenced me to elaborate my work.

I would also like to thank Dr. Amritanshu Pandey, Head, Dept. of Electronics Engineering, IIT (BHU), Varanasi, India, for providing the right academic environment. I sincerely thank my research performance evaluation committee (RPEC) members, Prof. V. N. Mishra and Dr. Shrawan Kumar Mishra, for their encouragement and insightful comments. Further, I am grateful to all the faculty members for their kind cooperation and encouragement during this journey. I would also like to acknowledge the valuable help of my colleagues, Mr. Jagadish, Mr. Ashok Kumar, Mr. Sumit, and Mr. Alok Tripathi, for their support and fruitful suggestions.

I am grateful to Dr. Sushant Mittal, an Applications Engineer at Synopsys India, for his valuable support and assistance during my Ph.D. research.

Finally, I wish to express my heartfelt gratitude to my father, Shri Virendra Prasad Choudhary, mother, Smt. Neelam Singh, brother, Ratnesh Singh, sisters, Ruchi Singh, wife Shipra Singh, and my son Raghav Singh for their love, prayers, blessings, and sacrifices that have educated and prepared me for my future.



ROOPESH SINGH

TABLE OF CONTENTS

CHAPTER-1	1
Introduction	1
1.1 Thesis Abstract.....	2
1.2 Introduction.....	5
1.3 Role of Synaptic Devices in Neuromorphic Computing.....	9
1.4 Ferroelectric-based Memory	12
1.5 Ferroelectric Memory Devices	16
1.6 FinFET Architecture-based Ferroelectric Memory: FeFinFET.....	19
1.7 Ferroelectric Memory as a Synaptic Device.....	24
1.8 FeFinFET-based Memory Cell	27
1.9 Magneto-Resistive based Memory.....	29
1.10 Recent Progress in Circuit and Device Techniques for Asymmetric Write Current Management in 1-bit STT-MRAM Cell.....	31
1.11 Asymmetric Transistors.....	33
1.12 Problem Statement	36
CHAPTER-2	39
Junctionless Accumulation-Mode SOI Ferroelectric FinFET for Synaptic Weights	39
2.1 Introduction:	40
2.2 Background, Device Structure, Operation, and Simulation Methodology	42
2.3 Fabrication Methodology and Comparison with Existing Process Flow	50
2.4 Transfer and Memory Cell Characteristics	51
2.5 Device Characterization and Discussion	55
2.6 CONCLUSION	62
CHAPTER-3	63
Memristive Ferroelectric FET for 1T-1R Nonvolatile Memory with Non-Destructive Readout	63
3.1 Introduction.....	64
3.2 Proposed Memristive Variant of FeFET (MFeFET)	68
3.3 Transfer And Memory Cell Characteristics	74
3.4 Performance Evaluation of 1T-1MFeFET Memory Cell Array Architecture Using NVSim...78	
3.5 CONCLUSION	80
CHAPTER-4	83
FinFET Fin-Trimming During Replacement Metal Gate for an Asymmetric Device Toward STT MRAM Performance Enhancement	83
4.1 Introduction.....	84
4.2 Calibration of Simulation Deck and Description of Approach	87

4.3 Selective Fin-Trimming and Gate-Stack Engineering for Asymmetric Performance	89
4.4 Results and Discussions	96
4.5 Conclusion.....	99
CHAPTER-5.....	101
Conclusion and Future Scope of Research.....	101
5.1 Chapter-wise Conclusion	103
5.2 Future Scope of Research	106
Author's Journal Publications	111
Author's Conference Publications	111
References.....	113

LIST OF FIGURES

Figure 1.1 Von Neumann architecture.....	7
Figure 1.2 Connection of two neurons in the human brain.	7
Figure 1.3 Neuromorphic architecture.....	9
Figure 1.4 Classification of conventional and emerging memory devices/technology.....	11
Figure 1.5 Polarization direction is changing by changing the direction of the voltage.....	13
Figure 1.6 Tetragonal structure and polarization (a) Up polarization (b) Down polarization.....	14
Figure 1.7 (a) The unit cell of a barium titanate (BaTiO_3) crystal illustrates two stable positions where the central Ti ion shifts upward or downward relative to the adjacent oxygen ion along the tetragonal symmetry axis. This displacement results in a net electric polarization oriented upward (state “0”) or downward (state “1”). (b) The Landau energy profile of the ferroelectric material depicts the polarization states. The two energy minima represent the stable polarization configurations. (c) The polarization vs electric field curve shows hysteresis nature.	16
Figure 1.8 Basic structure of early FeFET (a) ON-state (b) OFF-state.....	18
Figure 1.9 MFIS FeFET Structure.....	19
Figure 1.10 3-D structure of (a) Planar MOSFET (b) Bulk FinFET (c) SOI FinFET.	20
Figure 1.11 (a) 3-D structure of an n-MOS SOI FeFinFET. The 2-D cross-sectional views of the three-dimensional FinFET are depicted along the cut planes (b) C_1 and (c) C_2	21
Figure 1.12 Structure of 3-D JAM FeFinFET. A 2-D cross-sectional view of JAM FeFinFET along the plane (a) C_1 and (b) C_2	22
Figure 1.13 (a) Comparison of I_D - V_G curve of (a) JAM and conventional FinFET in log/linear scale, (b)-(c) shows the two-dimensional cross-section of the 3-D FinFET along the cut-plane C_1 . (b) Describes the electron density profile of JAM FinFET for biasing condition $V_{GS} = V_{DS} = 0.1$ V, (c) Describes the electron density profile of Conventional FinFET for biasing condition $V_{GS} = V_{DS} = 0.1$ V. (Here, we have used HfO_2 as a high- k dielectric material).....	23
Figure 1.14 FeFET-based pseudo crossbar array.	25
Figure 1.15 2T memory cell proposed in references (a) [107] (b) [108].	29
Figure 1.16 (a) 3-D Schematic of a 1-bit STT-MRAM cell. The MTJ is integrated with an access transistor in a 1T-1MTJ configuration (b) Standard connected STT-MRAM bit-cell.....	31
Figure 2.1 (a) 3-D NMOS SOI JAM FeFinFET structure, generated using process emulation. The two-dimensional cross-section of the 3-D JAM FeFinFET along (b) Cut-plane C_1 , (c) Cut-plane C_2	43
Figure 2.2 (a) 3-D NMOS SOI JAM FinFET structure, generated using process emulation. The	

two-dimensional cross-section of the 3-D JAM FinFET along (b) Cut-plane C_1 , (c) Cut-plane C_2	45
Figure 2.3 Calibration of the density-gradient model to precisely capture quantum-confinement in JAM FinFETs.	45
Figure 2.4 P-V calibration of FeCap with experimental data [140].	47
Figure 2.5 (a) JAM FeFinFET with contact at source/drain (b) 3-D contact structure, generated using structure editor in TCAD. (c) Two-dimensional cross-section of the contact along the cut-plane C_1	48
Figure 2.6 (a) I_D - V_G curve of JAM FeFinFET. (b) I_D - V_D curve of JAM FinFET without the ferroelectric material, here gate dielectric consists of $\text{HfO}_2 + \text{SiO}_2 = (1+0.75) \text{ nm} = 1.75 \text{ nm}$	48
Figure 2.7 TCAD simulated (a) Electron density due to down polarization, (b) Electron density due to up polarization, (c) Absolute polarization due to positive gate voltage, and (d) Absolute polarization due to negative gate voltage.	49
Figure 2.8 The proposed process flow of JAM FeFinFET.	51
Figure 2.9 Comparison of fabrication process.	51
Figure 2.10 I_D - V_G characteristics demonstrating the MW of (a) JAM FeFinFET, (b) Conventional FeFinFET.	53
Figure 2.11 (a) Comparison of conductance. (b) 2T JAM FeFinFET-based memory cell.	53
Figure 2.12 2T JAM FeFinFET memory cell transient waveform.	54
Figure 2.13 The simulated P-V curve of the proposed synaptic device for three different non-periodic asymmetric input signals, namely (a) case I, (b) case II, and (c) case III. Herein, $P_r = 2 \mu\text{C}/\text{cm}^2$, $P_s = 3 \mu\text{C}/\text{cm}^2$	56
Figure 2.14 (a) Applied asymmetric input gate pulse (b) Obtained P-V hysteresis spiral curve.	57
Figure 2.15 (a) Three different biasing voltages with the same initial and final voltage but different paths (b) History-dependent I_D - V_G characteristics of our proposed synaptic device.	58
Figure 2.16 The JAM FeFinFET I_D - V_G characteristics were obtained for each polarization state during (a) The program and (b) Erase voltages while conducting the read process, (c) The scheme used for biasing during the program (shown in green color) and erase (shown in red color) cycles.	58
Figure 2.17 Conductance vs pulse number characteristics of JAM FeFinFET at different gate voltage during read cycle after each prog-erase pulse [shown in Figure 2.16(c)], (a)-(b) At $V_{GS} = 0\text{V}$, (c)-(d) At $V_{GS} = 0.6\text{V}$, (e)-(f) At $V_{GS} = 1\text{V}$	60
Figure 2.18 (a) Waveform designed to program the 18-nm JAM FeFinFET to different states	

and then read the drain current (b) Measured $I_D - V_G$ characteristics after each program pulse, read after V_1 (Red color), after V_2 (Blue color), after V_3 (Black color) for each case. 61

Figure 3.1 FeFET memory cell proposed in (a) Ref. [107] (b) Proposed in this thesis. 66

Figure 3.2 (a) Comparison of MFeFET-based memory with other types of NVM memory. (b) 3-D visualization of 1T-1MFeFET.67

Figure 3.3 (a) 3-D n-MOS SOI FinFET structure, created through process emulation. The 2-D cross-section of the three-dimensional FinFET is shown along cut-plane (b) C_1 and (c) C_2 . . 69

Figure 3.4 (a) 3-D contact structure created with the structure editor in TCAD. (b) 2-D cross-sectional view of the contact along section C_1 . (c) The list of models is included in the calibrated Sentaurus TCAD deck. 71

Figure 3.5 (a) $I_D - V_G$ characteristics, along with a comparison with experimental data presented in [159]. (b) $I_D - V_D$ characteristics, along with a comparison with experimental data presented in [159]. 71

Figure 3.6 (a) 3-D n-MOS SOI FeFinFET structure, created through process emulation. (b) The 2-D cross-section of the three-dimensional FeFinFET across cut-plane C_1 , (c) P-V calibration of FeCap based on the experimental data presented in [140].72

Figure 3.7 Dependence of threshold voltage roll-off on H_{fin} for (a) Forward voltage sweep and (b) Reverse voltage sweep.....73

Figure 3.8 Dependence of threshold voltage roll-off on W_{fin} for (a) Forward voltage sweep, (b) Reverse voltage sweep.73

Figure 3.9 (a) Comparison of transfer characteristics of MFeFET for JAM and IM architecture (b) Proposed 1T- 1MFeFET-based NVM.....75

Figure 3.10 1T-1MFeFET memory cell transient waveform.77

Figure 3.11 Comparison of Bit line current in 1T-1MFeFET based memory cell for different bit line voltage during (a) Read ‘1’ (b) Read ‘0’79

Figure 3.12 Comparison of bit line current in 1T-1MFeFET based memory cell for different bit line voltage during (a) Read ‘1’ (b) Read ‘0’.79

Figure 3.13 (a) Representation of LRS and HRS in transfer characteristics of MFeFET. (b) NVsim Framework. 80

Figure 3.14 (a) and (b) Comparison of read latency for different memory capacities. 80

Figure 4.1 (a) A two-terminal MTJ device, (b) Standard connected STT-MRAM bit-cell, (c) Reverse connected STT-MRAM bit-cell. 85

Figure 4.2 (a) 3-D NMOS FinFET structure, generated using process emulation, (b) Impact of global fin trimming on NMOS and comparison with reported results from [137], (c) $I_D - V_G$

characteristics and comparison with experimental data reported in [159], (d) I_D - V_D characteristics and comparison with experimental data reported in [159]. 89

Figure 4.3 Proposed process flow of laterally-shifted selective fin-trimming and gate stack engineering for the asymmetric performance of FinFET. 91

Figure 4.4 (a) A typical layout for usual symmetric FinFET, depicting position of poly mask, fins and source/drain contact plug, (b) A modified layout to introduce asymmetry by asymmetric spacers [122] –a new mask layer is required to enable this fabrication, (c) proposed layout to introduce asymmetry in device. No new mask layer is required – poly mask is used with a lateral shift and a negative photoresist. Usage of this mask produces a structure, as shown in **Figure 4.3**.....92

Figure 4.5 (a) The 3-D asymmetric FinFET as fabricated from the process steps shown in **Figure 4.3** (b) A 2-D cross-section of the 3-D FinFET, along the cut-plane C_1 ; (c) The zoomed picture of fin-region of 2D FinFET. Partial fin trim and additional gate oxide in trimmed fin portion are shown; (d) A 2-D cross-section of the 3-D FinFET, along the cut-plane C_2 (a); (e) A zoomed picture of fin-region of 2-D FinFET, showing the reduced fin-height and additional gate oxide.93

Figure 4.6 Cross-section of the device (a) *Sym*: source/drain is grounded, (b) *Asym1*: source is grounded, (c) *Asym2*: drain is grounded. 94

Figure 4.7 (a) Total channel resistance(R_T) vs inverse of overdrive voltage ($1/V_{GS}-V_T$) of device *Asym1* for biasing condition is $V_{SS} = 0$ V and $V_{DS} = 0.7$ V, (b) Comparison of channel resistance (R_C) of devices *sym*, *Asym1*, and *Asym2*.95

Figure 4.8 Formation of inversion layer in channel for biasing condition (a) $V_{SS} = 0$ V & $V_{DS} = 0.7$ V, (b) $V_{SD} = 0.7$ V & $V_{DD} = 0$ V. 96

Figure 4.9 Cross-section of asymmetric device (a) Distribution of electric field when biasing condition $V_{SS} = 0$ V & $V_{DS} = 0.7$ V, i.e., *Asym1*, (b) Variation of electric field when biasing condition $V_{SD} = 0.7$ V & $V_{DD} = 0$ V i.e.,*Asym2*.97

Figure 4.10 Cross-section of the asymmetric device (a) Describes electron density profile for biasing condition $V_{SS} = 0$ V & $V_{DS} = 0.7$ V,i.e. *Asym1*, (b) Describes electron density profile for biasing condition $V_{SD} = 0.7$ V & $V_{DD} = 0$ V,i.e. *Asym2*.....97

Figure 4.11 (a) I_{ON} ratio (I_{ON} with drain ramped: I_{ON} with source ramped), vs. Fin trim amount [**Figure 4.5 (c)**], as a function of lateral-mask shift, for oxide fill in trimmed fin = 50%. More the fin-trim and lateral shift, more is asymmetry; (b) % reduction in I_{ON} with drain ramped to V_{DD} , as a function fin-trim and lateral mask shift. At 2 nm drain ramped, even though asymmetry is more, but % reduction in I_{ON} is also significant. 98

Figure 4.12 (a) I_{ON} ratio (I_{ON} with drain ramped: I_{ON} with source ramped), vs. Fin trim amount (Figure 4.5 (c)), as a function of lateral-mask shift, for oxide fill in trimmed fin = 100%. An attractive asymmetry of 27% is observed; (b) % reduction in I_{ON} with drain ramped to V_{DD} , as a function of fin-trim and lateral mask shift. 27% asymmetry comes at a price of even more reduced performance. 99

Figure 4.13 Comparison of C-V characteristics, with and without fin-trim. With the fin-trim case, a nearly 17% reduction in capacitance is observed. No fin-trim case capacitance is also representative of asymmetrically doped FinFET devices. 99

Figure 5.1 Thesis chapter outlines 102

LIST OF TABLES

Table 1.1 Comparison of existing asymmetric transistor.....	35
Table 2.1 TCAD simulation deck parameters [133],[134],[135].	45
Table 2.2 Experimentally calibrated model parameters of FeCap.	46
Table 3.1 Experimentally calibrated TCAD simulation deck parameters [133],[135],[134]. ...	70
Table 3.2 Experimentally validated model parameters for FeCap.	71
Table 3.3 Key parameter for MFeFET and MTJ.	78
Table 3.4 Benchmarking MFeFET with other nonvolatile memories.	81
Table 4.1 TCAD simulation deck parameters [159],[173].....	88
Table 4.2 Comparison of the asymmetric device proposed in [122] and in the present work.	100

LIST OF ABBREVIATIONS

Abbreviation	Details
CMOS	Complementary metal-oxide-semiconductor
SRAM	Static random-access memory
DRAM	Dynamic random-access memory
AI	Artificial intelligence
IOT	Internet of things
NVM	Non-volatile memory
FET	Field-effect transistor
FeFET	Ferroelectric field-effect transistor
FeFinFET	Ferroelectric fin field-effect transistor
MTJ	Magnetic Tunnel Junction
STT	Spin Transfer Torque
MRAM	Magneto-resistive random-access memory
JAM	Junctionless-accumulation-mode
MFeFET	Memristive ferroelectric field-effect transistor
RRAM	Resistive random-access memory
TCAD	Technology computer-aided design
PCM	Phase-change memory
PZT	Lead zirconate titanate
SBT	Strontium bismuth tantalate
AD	Asymmetrically doped
AS	Asymmetric spacers
HZO	Hafnium zirconium oxide
HKMG	High- k metal gate
ALD	Atomic layer deposition
FeRAM	Ferroelectric random-access memory
FeCap	Ferroelectric capacitor
BOX	Buried oxide
SOI	Silicon-on-insulator
MFIS	Metal-ferroelectric-insulator-semiconductor
p	Parallel
AP	Anti-Parallel
JL	Junctionless
JAM	Junctionless accumulation-mode field-effect transistors
DNN	Deep neural network
AM	Accumulation-mode
IM	Inversion-mode
PCRAM	Phase-change random-access memory
STDTP	Spike-timing-dependent plasticity

LTD	Long-term depression
LTP	Long-term potentiation
BEOL	Back-end-of-line
FEOL	Fack-end-of-line
S/D	Source/Drain
BTBT	Band-to-band tunneling
SRH	Shockley-read-hall recombination
IALMob	Inversion and accumulation layer mobility
PhuMob	Philips unified mobility model
TAT	Trap assisted tunneling
LiM	Logic-in-Memory
PL	Pinned Layer
FL	Free Layer
CiM	Compute-in-memory
SOT	Spin-orbit Torque
RMG	Replacement metal gate
MLCS	Multilevel cells
RL	Read line
WL	Write line
SL	Select line
BL	Bit line
RC	Reverse connected
SC	Standard connected

LIST OF SYMBOLS

Symbol	Abbreviation
V_{th}	Threshold voltage
T_C	Curie temperature
E	Electric field
P	Polarization
P_r	Remnant polarization
P_s	Saturation polarization
E_C	Coercive field
G	Gibs free energy
P	Parallel
AP	Anti-parallel
R_T	Total resistance
R_{slcd}	Silicide resistance
R_{plug}	Plug resistance
R_S	Source resistance
R_D	Drain resistance
V_{GG}	Gate voltage
V_{DS}	Drain to source voltage
T_{BOX}	Buried oxide thickness
V_{GS}	Gate to source voltage
V_{thH}	High threshold voltage
V_{thL}	Low threshold voltage
I_D	Drain current
W_{fin}	Fin width
H_{fin}	Fin height
I_{OFF}	OFF current
I_{ON}	ON current
C_{gg}	Gate capacitance

